

---

# L-[1-<sup>11</sup>C]-Tyrosine PET to Evaluate Response to Hyperthermic Isolated Limb Perfusion for Locally Advanced Soft-Tissue Sarcoma and Skin Cancer

Robert J. van Ginkel, Annemieke C. Kole, Omgo E. Nieweg, Willemina M. Molenaar, Jan Pruim, Heimen Schraffordt Kooops, Willem Vaalburg and Harald J. Hoekstra

Department of Surgical Oncology, PET Center and Department of Pathology, Groningen University Hospital, Groningen, The Netherlands; and Department of Surgery, The Netherlands Cancer Institute, Amsterdam, The Netherlands

---

PET with L-[1-<sup>11</sup>C]-tyrosine (TYR) was investigated in patients undergoing hyperthermic isolated limb perfusion (HILP) with recombinant tumor necrosis factor alpha (rTNF- $\alpha$ ) and melphalan for locally advanced soft-tissue sarcoma and skin cancer of the lower limb. **Methods:** Seventeen patients (5 women, 12 men; age range 24–75 y; mean age 52 y) were studied. TYR PET studies were performed before HILP and 2 and 8 wk afterwards. The protein synthesis rates (PSRs) in nanomoles per milliliter per minute were calculated. After final PET studies, tumors were resected and pathologically examined. Patients with pathologically complete responses (pCR) showed no viable tumors after treatment. Those with pathologically partial responses (pPR) showed various amounts of viable tumors in the resected tumor specimens. **Results:** Six patients (35%) showed a pCR and 11 patients (65%) showed a pPR. All tumors were depicted as hot spots on PET studies before HILP. The PSR in the pCR group at 2 and 8 wk after perfusion had decreased significantly ( $P < 0.05$ ) in comparison to the PSR before HILP. A significant difference was found in PSR between the pCR and pPR groups at 2 and 8 wk ( $P < 0.05$ ). Median PSR in nonviable tumor tissue was 0.62 and ranged from 0.22 to 0.91. With a threshold PSR of 0.91, sensitivity and specificity of TYR PET were 82% and 100%, respectively. The predictive value of a PSR  $> 0.91$  for having viable tumor after HILP was 100%, whereas the predictive value of a PSR  $\leq 0.91$  for having nonviable tumor tissue after HILP was 75%. The 2 patients in the pPR groups with a PSR  $< 0.91$  showed microscopic islets of tumor cells surrounded by extensive necrosis on pathological examination. **Conclusion:** Based on the calculated PSR after HILP, TYR PET gave a good indication of the pathological outcome. Inflammatory tissue after treatment did not interfere with viable tumor on the images, suggesting that it may be worthwhile to pursue TYR PET in other therapy evaluation settings.

**Key Words:** PET; <sup>11</sup>C-tyrosine; hyperthermic isolated limb perfusion; tumor necrosis factor; sarcoma; melanoma

**J Nucl Med 1999; 40:262–267**

---

**D**ifferent metabolic processes such as glycolysis, protein synthesis, uptake of disaccharides and transamination are enhanced in tumors when compared to normal tissues. PET enables visualization and quantification of metabolic processes in vivo. <sup>18</sup>F-labeled 2-fluoro-2-deoxy-D-glucose (FDG) is the most commonly used radiopharmaceutical for PET and has proven to be of value to visualize various types of solid tumors, to indicate the malignancy grade and to detect locally recurrent disease (1–4). Various clinical reports suggest the feasibility of FDG PET to assess tumor response to radiotherapy and chemotherapy (5–7). A limitation of FDG PET in therapy evaluation is the inability to differentiate between viable tumor tissue and inflammatory tissue (8–10). Therefore, there is a need for alternatives. Ishiwata et al. (11) have shown that the uptake of amino acids is high in tumor tissue due to an increased protein synthesis rate (PSR). Amino acids play a minor role in the metabolism of inflammatory cells, mainly neutrophils, compared to FDG. Most amino acid PET studies have been performed with L-[methyl-<sup>11</sup>C]-methionine (MET) (12–14). MET reflects amino acid uptake rather than protein synthesis, because it is involved in other metabolic pathways such as transmethylation and polyamine synthesis (15,16). The complicated metabolism of MET has made it impossible to create a precise metabolic model. Carboxyl-labeled amino acids, such as L-[1-<sup>11</sup>C]-tyrosine (TYR), L-[1-<sup>11</sup>C]-methionine and L-[1-<sup>11</sup>C]-leucine, appear to be more appropriate compounds to determine protein synthesis in tumors (16,17). The main metabolite of these amino acids is <sup>11</sup>CO<sub>2</sub>, which is rapidly cleared from tissue and exhaled and does not contribute to the PET-measured <sup>11</sup>C radioactivity in tumor tissue.

A model was developed to determine the PSR in tumor tissue using TYR (18). Initial results in patients with brain tumors have been published previously (19). Kole et al. (20) reported a high uptake of TYR and, as a consequence, a high PSR in various types of malignancies and low uptake in benign lesions. PET with TYR may be of value in the assessment of the response of malignant tumors to therapy,

---

Received Feb. 24, 1998; accepted May 27, 1998.

For correspondence or reprints contact: Robert J. van Ginkel, MD, Department of Surgery, Division of Surgical Oncology, Groningen University Hospital, P.O. Box 30.001, Groningen 9700 RB, The Netherlands.

because a decrease in tissue viability may result in a decrease in PSR. Hyperthermic isolated limb perfusion (HILP) with recombinant tumor necrosis factor alpha (rTNF- $\alpha$ ) and melphalan can usually prevent amputation in patients with locally advanced soft-tissue sarcoma or extensive local regional melanoma (21,22). The aim of this study was to investigate PET with TYR in patients undergoing HILP for locally advanced soft-tissue sarcoma and skin cancer and to correlate PET findings with histology before and after treatment.

## MATERIALS AND METHODS

### Patients

Seventeen patients (5 women, 12 men; age range 24–75 y; mean age 52 y) with biopsy-proven soft-tissue sarcoma or melanoma participated in the study approved by the Medical Ethical Committee of the institute. Informed consent was obtained from each patient. Ten patients presented with newly diagnosed soft-tissue sarcoma, 2 patients presented with local recurrence of soft-tissue sarcoma previously treated with surgery alone, 4 patients presented with melanoma and 1 patient presented with squamous cell carcinoma. All tumors were located in the lower limb. The diagnosis of the tumors was determined in a standard fashion, and soft-tissue sarcomas were graded according to Coindre et al. (23). All tumors were considered primarily irresectable because of size, multicentricity in the limb or fixation to the neurovascular bundle or bone. Median tumor size was 10 cm (range 3–25 cm). Patients and tumor characteristics are summarized in Table 1.

### Methods

The perfusion technique used at the Groningen University Hospital is based on the technique developed by Creech et al. (24) and has been described in detail previously (22). Briefly, after cannulation of the vessels of the perfused limb, a tourniquet is placed at the base to prevent systemic leakage. The limb is perfused

with 4 mg rTNF- $\alpha$  (Boehringer, Ingelheim, Germany) administered directly intraarterially, followed 30 min later by 10 mg/L volume melphalan (Burrroughs Wellcome, London, England). Perfusion is carried out for 90 min under hyperthermic conditions (39–40°C). Preventive measures to cope with the expected side effects caused by leakage consist of fluid loading and administration of vasoactive amines. After HILP, patients are mechanically ventilated until they are hemodynamically stable and receive intensive care management as described by Zwaveling et al (25).

Approximately 8 wk after perfusion (median 66 d, range 27–125 d), the residual tumor masses were excised and pathologically examined. The tumor remnants were measured in three dimensions, and the percentage of necrosis was estimated. Representative tumor sections were taken, encompassing macroscopically different tumor areas including necrosis. As a general rule, one section per centimeter diameter, with a minimum of three, was taken. Based on an integration of gross and microscopic findings, a final estimate of the percentages of viable and necrotic or regressive tumor was made. If possible, macroscopic examination and tissue sampling were performed on the basis of the latest PET images. The results were classified as either pathologically complete response (pCR) or pathologically partial response (pPR) when remaining viable tumor was noted.

### PET Imaging

Patients were scheduled for three PET studies: shortly before perfusion ( $n = 17$ , median 10 d, range 1–23 d), 2 wk after perfusion ( $n = 14$ , median 16 d, range 12–23 d) and shortly before resection of residual tumor tissue ( $n = 15$ , median 55 d, range 47–68 d after perfusion). TYR was produced by a modified microwave-induced Bücherer-Strecker synthesis (26), with a radiochemical purity of more than 99%. PET sessions were performed using an ECAT 951/31 PET camera (Siemens/CTI, Knoxville, TN).

All patients fasted for at least 8 h before the investigation. Serum tyrosine levels were measured before each PET session and were found to be normal (mean 0.053 mmol/L, range 0.028–0.1 mmol/L).

**TABLE 1**  
Tumor Characteristics

Patient no.	Histology	Site	Grade	No. of lesions	Largest diameter (MRI) (cm)
1	Melanoma	Recurrent	Lower leg	na	3.5
2	Squamous cell carcinoma	Primary	Foot	na	6.0
3	Clear cell carcinoma	Primary	Lower leg	3	10.0
4	Melanoma	Recurrent	Lower leg	na	4.0
5	Leiomyosarcoma	Primary	Lower leg	3	12.5
6	Melanoma	Primary	Lower leg	na	7.0
7	Synoviosarcoma	Primary	Popliteal fossa	2	4.0
8	Fibrosarcoma	Primary	Knee	1	3.0
9	Synoviosarcoma	Recurrent	Lower leg	2	9.0
10	Haemangiopericytoma	Primary	Popliteal fossa	2	15.0
11	Malignant fibrous histiocytoma	Primary	Thigh	3	23.0
12	Angiosarcoma	Primary	Lower leg	3	12.5
13	Extraosseous osteosarcoma	Primary	Thigh	3	25.0
14	Myxoid liposarcoma	Primary	Thigh	1	8.0
15	Myxoid liposarcoma	Primary	Popliteal fossa	2	11.0
16	Malignant fibrous histiocytoma	Primary	Thigh	2	10.0
17	Melanoma	Primary	Toe	na	3.0

na = not applicable.

L). A 20-gauge needle was inserted into the radial artery under local anesthesia. In the contralateral arm, an intravenous cannula was inserted in the cephalic vein for the injection of TYR. The patients were positioned supine in the camera, with the tumor in the field of view based on physical examination.

After attenuation scanning using a  $^{68}\text{Ge}/^{68}\text{Ga}$  source, we administered a mean dose of 322 MBq (range 126–381 MBq [8.7 mCi, range 3.4–10.3 mCi]) TYR intravenously over 1 min. Dynamic images were acquired from the time of injection following a dynamic protocol (ten 0.5 min, three 5 min, three 10 min) for a total duration of 50 min. Simultaneously, 2-ml blood samples were taken from the arterial canula (time points 0.25, 0.5, 0.75, 1.0, 1.25, 1.5, 1.75, 2.25, 2.45, 3.75, 4.75, 7.5, 12.5, 17.5, 25.0, 35.0 and 45.0 min postinjection). The blood samples were centrifuged and plasma activity of TYR, the  $^{11}\text{C}$ -labeled  $\text{CO}_2$  and protein levels were measured by high-performance liquid chromatography (HPLC). The duration of the imaging procedure was approximately 2.5 h.

### Data Analysis

Images were displayed in coronal, sagittal and transaxial projections on a computer display using standard ECAT software and were interpreted independently by two experienced physicians. To determine tumor PSR, one must first define the tumor in all relevant tomographic planes of the study. Usually this is done by placing regions of interest (ROIs) in each plane, matching the size of the tumor as outlined by MRI. The tissue time-activity curves obtained from these ROIs can be averaged and the average PSR can be calculated. Because this technique is rather laborious, an alternative method was developed at our institute. By using the same activity threshold as the one used to define the ROI, we selected all voxels in the study above this threshold. For each analysis, a fixed percentage of 95% was used. The corresponding activity was summed and the average time-activity curve and total

volume were obtained. The advantage of this approach is that the analysis of the whole tumor is performed quickly and simply, and the results are identical to those of the ROI method. Parts of the tumor that do not accumulate TYR are ignored by this method. By combining this averaged time-activity data with the plasma input data (corrected for  $^{11}\text{CO}_2$  and  $^{11}\text{C}$ -proteins), we calculated the average PSR in nanomoles per milliliter tumor tissue per minute using the modified Patlak analysis as described previously (18). The PSR in contralateral normal tissue was calculated using a ROI technique. A tumor-to-nontumor ratio (T/N ratio) was calculated from the PSR in tumor tissue and the PSR in contralateral normal tissue. The change in PSR after perfusion was related to the preperfusional value and was expressed as a percentage of basal value.

### Statistical Analysis

The statistical procedures included a two-factor experiment with repeated measures on one factor to compare PSR between measures and groups. Analyses were performed on data sets corrected for missing data according to Winer (27). Post hoc comparison was made with Student *t* tests.  $P < 0.05$  was considered significant.

### RESULTS

PET results and pathological response for each patient are summarized in Table 2. Pathological examination of the residual tumor mass showed no viable tumors in 6 patients (pCR 35%), 3 of whom had melanomas. In 11 patients, variable amounts of viable tumors were found at pathological examination (pPR 65%). Forty-six of the scheduled 51 PET studies were completed (90%). Five PET studies were not performed due to patient-related problems. All tumors

**TABLE 2**  
PET Results and Pathological Response

Patient no.	Before HILP			2 weeks after HILP			8 weeks after HILP			Response	Pathological evaluation	
	PSR tumor	PSR contralat	T/N ratio	PSR tumor	PSR contralat	T/N ratio	PSR tumor	PSR contralat	T/N ratio		% viable tumor	Macro-/microscopic view
1	2.45	0.14	17.5	0.17	0.14	1.2	0.22	0.41	0.5	pCR	0	Rim with inflammatory tissue
2	3.51	0.15	23.4	1.02	0.16	6.4	0.91	0.20	4.6	pCR	0	Inflammatory tissue
3	2.53	0.43	5.9	np	np	np	0.50	0.31	1.6	pCR	0	Inflammatory tissue
4	2.06	0.40	5.2	0.74	0.26	2.9	np	np	np	pCR	0	Inflammatory tissue
5	2.13	0.41	5.2	0.71	0.23	3.1	0.85	0.20	4.3	pCR	0	Rim with inflammatory tissue
6	1.31	0.40	3.3	0.62	0.27	2.3	0.35	0.21	1.7	pCR	0	Inflammatory tissue
7	2.06	0.24	8.6	1.39	0.43	3.2	0.48	0.29	1.7	pPR	<10	Microscopic islets of viable tumor
8	1.76	0.25	7.0	0.64	0.26	2.5	0.80	0.21	3.8	pPR	<10	Microscopic islets of viable tumor
9	0.92	0.33	2.8	np	np	np	0.99	0.32	3.1	pPR	<10	Microscopic islets of viable tumor
10	2.00	0.23	8.7	2.30	0.30	7.7	1.46	0.22	6.6	pPR	<10	Areas of viable tumor
11	2.30	0.26	8.9	1.26	0.18	7.0	2.31	0.16	14.4	pPR	<10	Areas of viable tumor
12	5.27	0.25	21.1	2.79	0.18	15.5	np	np	np	pPR	<10	Areas of viable tumor
13	1.68	0.17	9.9	np	np	np	3.91	0.48	8.2	pPR	<20	Rim with viable tumor
14	0.73	0.24	3.4	1.61	0.47	3.4	1.83	0.48	3.8	pPR	<50	Areas of viable tumor
15	0.64	0.24	2.7	1.35	0.33	4.1	2.13	0.60	3.6	pPR	<50	Areas of viable tumor
16	2.90	0.46	6.3	1.47	0.43	3.4	2.48	0.31	8.0	pPR	<50	Areas of viable tumor
17	1.61	0.24	6.7	1.24	0.09	13.8	0.94	0.08	11.8	pPR	<50	Viable tumor

HILP = hyperthermic isolated limb perfusion; PSR = protein synthesis rate; contralat = contralateral normal tissue; T/N = tumor-to-nontumor; pCR = pathologically complete response; np = not performed; pPR = pathologically partial response.

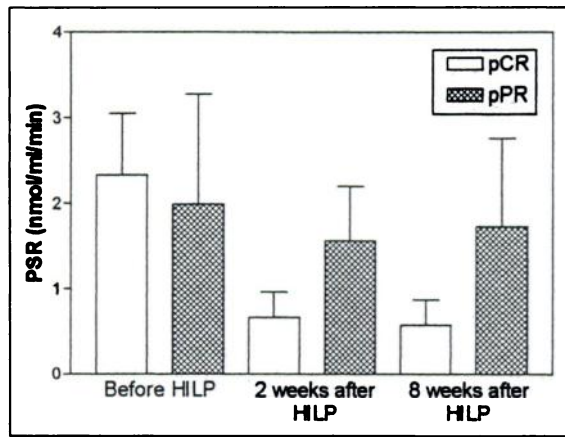


**FIGURE 1.** Protein synthesis rate (PSR) of tumor with SD before, 2 and 8 wk after perfusion. Two and 8 wk after perfusion, PSR in pathologically complete response (pCR) group decreased significantly ( $P < 0.05$ ) in contrast with PSR in pathologically partial response (pPR) group. Significant difference was found in PSR between pCR and pPR groups at 2 and at 8 wk ( $P < 0.05$ ). HILP = hyperthermic isolated limb perfusion.

were depicted as a hot spot on the PET study before HILP with variable degrees of TYR accumulating parts (T/N ratio  $> 1.00$  in all patients). Preperfusion PSR in the patients who ultimately went on to have a pCR was not significantly different from the PSR in the pPR group (Fig. 1). Analysis of the PET images at 2 and 8 wk after perfusion showed a decrease of TYR accumulating parts in all pCR patients. The PSR in the pCR group had decreased significantly at 2 and 8 wk after perfusion compared with preperfusional values ( $P < 0.05$ ) in contrast to the PSR in the pPR group. A significant difference was found in PSR between the pCR and pPR groups at 2 and at 8 wk ( $P < 0.05$ ). The most substantial decrease in PSR occurred within 2 wk after perfusion. Figure 2 illustrates the succeeding PET studies in patient 11. After an initial decrease in PSR at 2 wk, a renewed outgrowth of the tumor was observed at 8 wk after perfusion. Necrosis within the tumor was visualized as a cold spot. In this patient, TYR PET indicated the need for an early resection of the tumor, because perfusion did not seem to have the desired result. Pathological examination revealed areas of viable tumor that encompassed less than 10% of the total tumor volume.

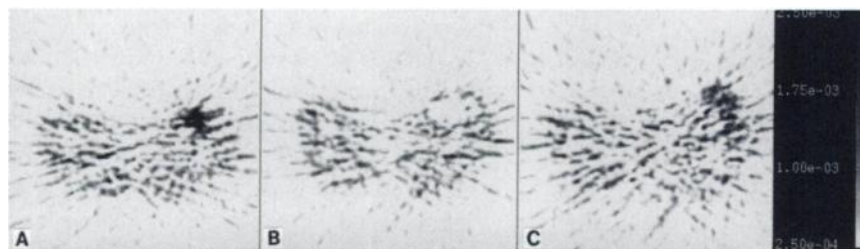


**FIGURE 2.** Transverse PET image of patient with malignant fibrous histiocytoma of thigh (patient 11). (A) Before perfusion, tumor is clearly depicted as heterogeneous mass with PSR of 2.30 nmol/mL/min. (B) After initial reduction in PSR (1.26) at 2 wk after perfusion, malignant fibrous histiocytoma showed renewed growth (PSR 2.31) at (C) 8 wk after perfusion. Gray scale equates particular hue to particular PSR in micromole per milliliter per minute.

The median PSR in contralateral muscle tissue was 0.28 and ranged from 0.08 to 0.60. PSR in tumor tissue was higher than in the corresponding contralateral normal tissue ( $P < 0.05$ ). Median PSR in nonviable tumor tissue was 0.62 and ranged from 0.22 to 0.91. With a threshold PSR of 0.91, the highest value obtained from nonviable tumor tissue, the sensitivity and specificity of TYR PET after HILP treatment were 82% and 100%, respectively. The predictive value of a PSR  $> 0.91$  for viable tumor after HILP was 100%, whereas the predictive value of a PSR  $\leq 0.91$  for nonviable tumor tissue after HILP was 75% (Fig. 3). The two patients in the pPR group with a PSR  $< 0.91$ , patients 8 and 9, showed microscopic islets of tumor cells surrounded by extensive necrosis on pathological examination. With a threshold PSR of 0.48, the lowest value obtained from viable tumor tissue, the sensitivity and specificity of TYR PET after HILP treatment were 100% and 33%, respectively. The predictive values for viable and nonviable tumor tissue after HILP were 73% and 100%, respectively.

Figure 4 shows the percentage of basal value of the tumor after perfusion. All patients in the pCR group showed a reduction of PSR, whereas some pPR patients showed a reduction and others an increase in PSR after perfusion. The reduction in the pCR group was significant at 2 and 8 wk after perfusion. However, based on a certain percentage of reduction of basal value, no assumption could be made as to whether or not the individual patient showed a pCR or a pPR.

Two different histopathological groups could be distinguished after perfusion: nonviable tumor tissue, corresponding with inflammatory tissue, and viable tumor tissue. Figure 5 shows the PSR in these two different histopathological groups compared with the PSR in normal contralateral muscle. The average PSR in inflammatory tissue was significantly lower than the PSR values in viable tumor tissue ( $P < 0.05$ ).

## DISCUSSION

PET has made it possible to study biochemical changes of cancer tissue and the effect of treatment on metabolism in vivo. This study demonstrates a significant decline in the protein metabolism of locally advanced soft-tissue sarcomas and skin cancer with a pathologically complete response

	PA Viable	PA Nonviable	Total
PET Viable	9	0	9
PET Nonviable	2	6	8
Total	11	6	17

**FIGURE 3.** Cross-tabulation with threshold PSR of 0.91. Sensitivity and specificity of TYR PET were 82% and 100%, respectively. Predictive value for viable tumor after HILP was 100%, whereas predictive value for nonviable tumor tissue after HILP was 75%. Two patients in the pPR group with PSR < 0.91 showed microscopic islets of tumor cells surrounded by extensive necrosis on pathological examination. PA = pathology.

after HILP with rTNF- $\alpha$  and melphalan. These changes were already evident within 2 wk. In patients with a pPR, this decrease was not significant. These findings are similar to the results of a previous study performed in the same manner with FDG (9). With TYR PET, however, there was a significant difference at 2 and 8 wk in PSR between the pCR and pPR groups, a finding that was not observed with FDG PET. That previous finding may have been caused by the fact that FDG is also accumulated by inflammatory tissue, resulting in an overlap in glucose metabolism between viable tumor and inflammatory tissue. In this study, TYR was also accumulated by inflammatory tissue that existed after HILP but was accumulated significantly less than in viable tumor tissue. Because TYR can better discriminate between viable tumor tissue and inflammatory tissue than FDG, TYR is a more reliable technique to evaluate treatment response. The major question for clinicians is the exact timing for surgical resection after HILP, because the tumoricidal effect of HILP seems to be time related. If the threshold PSR of 0.91 was exceeded 8 wk after

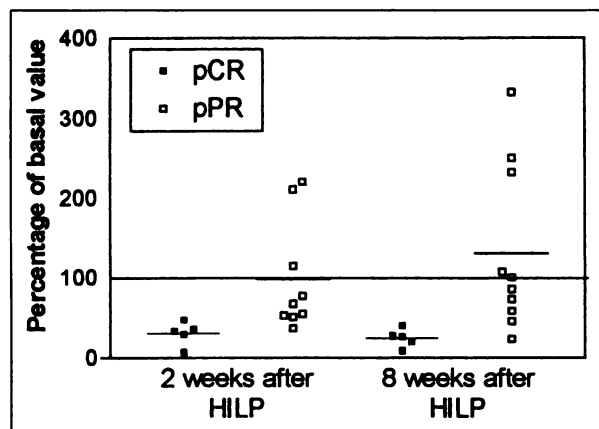


**FIGURE 4.** Percentage of basal value of tumor for all patients 2 and 8 wk after perfusion. pCR = pathologically complete response; pPR = pathologically partial response; HILP = hyperthermic isolated limb perfusion.

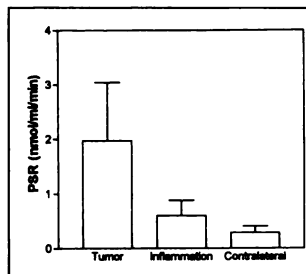


**FIGURE 5.** Protein synthesis rate (PSR) in viable tumor, inflammatory and contralateral normal tissue. PSR in viable tumor tissue was significantly higher than inflammatory tissue ( $P < 0.05$ ).

HILP, we could with certainty predict that viable tumor was still present and surgical resection of the tumor remnants was indicated. However, when resection was omitted with a PSR less than 0.91, there was a 25% chance of leaving microscopic islets of tumor tissue. The resolution of the PET camera may be the limiting factor in detecting these microscopic islets of viable tumor, although it remains questionable if these small amounts of tumor tissue surrounded by avascular necrosis can lead to a local recurrence. Instead of surgical resection, these patients could possibly also be treated with external beam radiotherapy and monitored closely for development of local recurrence. Leaving residual tumor mass was safe when PSR was lower than 0.48 after HILP.

Before perfusion, there was no significant difference in PSR between the patients in the pCR and pPR groups. This was in contrast with the results of the FDG study where we found a significant difference in glucose consumption before perfusion between both groups (9). So TYR cannot be used to predict the likelihood of a response to HILP. For FDG, we also found a correlation between tumor malignancy grade and the level of glucose metabolism (3). This is not the case for the protein synthesis of the different grades of soft-tissue sarcomas in this study, but the number of patients is small. This difference between FDG and TYR may be explained by the fact that FDG is trapped inside the cell as a result of an increased level of glucose transporters on the cell membrane (28). FDG accumulates as it reaches its end in its metabolic pathway as FDG-6-phosphate; the more glucose transporters there are on the cell membrane, the more FDG is incorporated in the cell, corresponding with a high malignancy grade. TYR, not hampered by an anorganic isotope, continues its metabolic pathway and is not accumulated in the cell.

Combining the results of this study with the results of our previous FDG study, it is tempting to state that FDG PET should be performed before HILP to identify patients who will most likely benefit from this treatment and that TYR PET should be performed 8 wk after HILP to evaluate the outcome of the therapy. However, our results should be interpreted with caution because this patient population included a small group of heterogeneous soft-tissue sarcomas and skin cancers and only large tumors were included. Additional data are needed on TYR PET in more patients with other tumor types treated with other chemotherapeutic agents and with pathological examination as the gold standard.

## CONCLUSION

This study demonstrates that TYR PET indicates the pathologic tumor response to chemotherapy in an investigational setting used with HILP with rTNF- $\alpha$  and melphalan for locally advanced tumors. Based on the calculated PSR after perfusion, a good indication was found toward the pathological outcome. Inflammatory tissue after treatment did not interfere with viable tumor on the images, suggesting that it may be worthwhile to pursue TYR PET in other therapy evaluation settings.

## REFERENCES

1. Conti PS, Lilien DL, Hawley K, Keppler J, Grafton ST, Bading JR. PET and [ $^{18}\text{F}$ ]-FDG in oncology: a clinical update. *Nucl Med Biol.* 1996;23:717-735.
2. Rigo P, Paulus P, Kaschten BJ, et al. Oncological applications of positron emission tomography with fluorine-18 fluorodeoxyglucose. *Eur J Nucl Med.* 1996;23:1641-1674.
3. Nieweg OE, Pruijm J, van Ginkel RJ, et al. Fluorine-18-fluorodeoxyglucose PET imaging of soft-tissue sarcoma. *J Nucl Med.* 1996;37:257-261.
4. Kole AC, Nieweg OE, van Ginkel RJ, et al. Detection of local recurrence of soft-tissue sarcoma with positron emission tomography using [ $^{18}\text{F}$ ]fluorodeoxyglucose. *Ann Surg Oncol.* 1997;4:57-63.
5. Findlay M, Young H, Cunningham D, et al. Noninvasive monitoring of tumor metabolism using fluorodeoxyglucose and positron emission tomography in colorectal cancer liver metastases: correlation with tumor response to fluorouracil. *J Clin Oncol.* 1996;14:700-708.
6. Jones DN, McCowage GB, Sostman HD, et al. Monitoring of neoadjuvant therapy response of soft-tissue and musculoskeletal sarcoma using fluorine-18-FDG PET. *Blood.* 1996;37:1438-1444.
7. Lindholm P, Leskinen Kallio S, Grenman R, et al. Evaluation of response to radiotherapy in head and neck cancer by positron emission tomography and [ $^{11}\text{C}$ ]methionine. *Int J Radiat Oncol Biol Phys.* 1995;32:787-794.
8. Kubota R, Yamada S, Kubota K, Ishiwata K, Tamahashi N, Ido T. Intratumoral distribution of fluorine-18-fluorodeoxyglucose in vivo: high accumulation in macrophages and granulation tissues studied by microautoradiography. *J Nucl Med.* 1992;33:1972-1980.
9. van Ginkel RJ, Hoekstra HJ, Pruijm J, et al. FDG PET to evaluate response to hyperthermic isolated limb perfusion for locally advanced soft tissue sarcoma. *J Nucl Med.* 1996;37:984-990.
10. Lewis PJ, Salama A. Uptake of fluorine-18-fluorodeoxyglucose in sarcoidosis. *J Nucl Med.* 1994;35:1647-1649.
11. Ishiwata K, Vaalburg W, Elsinga PH, Paans AM, Woldring MG. Metabolic studies with L-[1- $^{14}\text{C}$ ]tyrosine for the investigation of a kinetic model to measure protein synthesis rates with PET. *J Nucl Med.* 1988;29:524-529.
12. Schober O, Meyer GJ, Duden C, et al. Amino acid uptake in brain tumors using positron emission tomography as an indicator for evaluating metabolic activity and malignancy. *Rofo Fortschr Geb Rontgenstr Nuklearmed.* 1987;147:503-509.
13. Derlon JM, Bourdet C, Bustany P, Chatel M, Theron J, Darcel FSA. [ $^{11}\text{C}$ ]L-methionine uptake in gliomas. *Neurosurgery.* 1989;25:720-728.
14. Lilja A, Lundqvist H, Olsson Y, Spannare B, Gullberg P, Langstrom B. Positron emission tomography and computed tomography in differential diagnosis between recurrent or residual glioma and treatment-induced brain lesions. *Acta Radiol.* 1989;30:121-128.
15. Daemen BJ, Elsinga PH, Ishiwata K, Paans AM, Vaalburg W. A comparative PET study using different  $^{11}\text{C}$ -labelled amino acids in Walker 256 carcinosarcoma-bearing rats. *Int J Rad Appl Instrum.* 1991;18:197-204.
16. Ishiwata K, Vaalburg W, Elsinga PH, Paans AM, Woldring MG. Comparison of L-[1- $^{11}\text{C}$ ]methionine and L-methyl-[ $^{11}\text{C}$ ]methionine for measuring in vivo protein synthesis rates with PET. *J Nucl Med.* 1988;29:1419-1427.
17. Bolster JM, Vaalburg W, Paans AM, et al. Carbon-11 labelled tyrosine to study tumor metabolism by positron emission tomography (PET). *Eur J Nucl Med.* 1986;12:321-324.
18. Willemsen ATM, van Waarde A, Paans AM, et al. In vivo protein synthesis rate determination in primary or recurrent brain tumors using L-[1- $^{11}\text{C}$ ]tyrosine and PET. *J Nucl Med.* 1995;36:411-419.
19. Pruijm J, Willemsen AT, Molenaar WM, et al. Brain tumors: L-[1- $^{11}\text{C}$ ]tyrosine PET for visualization and quantification of protein synthesis rate. *Radiology.* 1995;197:221-226.
20. Kole AC, Pruijm J, Nieweg OE, et al. PET with L-[1-carbon-11]-tyrosine to visualize tumors and measure protein synthesis rates. *J Nucl Med.* 1997;38:191-195.
21. Lienard D, Ewalenko P, Delmotte JJ, Renard N, Lejeune FJ. High-dose recombinant tumor necrosis factor alpha in combination with interferon gamma and melphalan in isolation perfusion of the limbs for melanoma and sarcoma. *J Clin Oncol.* 1992;10:52-60.
22. Eggermont AMM, Schraffordt Koops H, Lienard D, et al. Isolated limb perfusion with high-dose tumor necrosis factor-alpha in combination with interferon-gamma and melphalan for nonresectable extremity soft tissue sarcomas: a multicenter trial. *J Clin Oncol.* 1996;14:2653-2665.
23. Coindre JM, Trojani M, Contesso G, et al. Reproducibility of a histopathologic grading system for adult soft tissue sarcoma. *Cancer.* 1986;58:306-309.
24. Creech O, Krementz ET, Ryan RF, Winblad JN. Chemotherapy of cancer: regional perfusion utilizing an extra-corporeal circuit. *Ann Surg.* 1958;148:616-632.
25. Zwaveling JH, Maring JK, Clarke FL, et al. High plasma tumor necrosis factor (TNF)-alpha concentrations and a sepsis-like syndrome in patients undergoing hyperthermic isolated limb perfusion with recombinant TNF-alpha, interferon-gamma, and melphalan. *Crit Care Med.* 1996;24:765-770.
26. Giron C, Luurtsema G, Vos MG, Elsinga PH, Visser GM, Vaalburg W. Microwave-induced preparation of  $^{11}\text{C}$ -amino-acids via NCA-Bücherer-Strecker synthesis. *J Lab Compnd Radiopharm.* 1995;37:752-754.
27. Winer BJ. *Statistical Principles in Experimental Design.* New York, NY: McGraw Hill; 1971.
28. Brown RS, Wahl RL. Overexpression of Glut-1 glucose transporter in human breast cancer. *Cancer.* 1993;72:2979-2985.